



Effect of reducing agent (C_3H_6 , CO, H_2) on the NO_x conversion and selectivity during representative lean/rich cycles over monometallic platinum-based NSR catalysts. Influence of the support formulation

Liliana Masdrag, Xavier Courtois*, Fabien Can, Daniel Duprez

Université de Poitiers-CNRS, Institut de Chimie des Milieux et des Matériaux de Poitiers (IC2MP), UMR 7285, 4 rue Michel Brunet, F-86022 Poitiers Cedex, France

ARTICLE INFO

Article history:

Received 2 October 2012

Received in revised form 17 May 2013

Accepted 11 June 2013

Available online 20 June 2013

Keywords:

NO_x reduction

Selectivity

N_2O

NSR

LNT

ABSTRACT

NO_x storage reduction efficiency was investigated on a Pt–10% BaO/Al_2O_3 model catalyst using a complex gas feed including reductants and oxidants in both lean and rich mixtures. Three representative reductants have been studied, separately and blended: C_3H_6 , CO, H_2 and $C_3H_6 + CO + H_2$. The influence of each reductant was evaluated with a special consideration to the N_2O selectivity. The reductant/oxidant ratio was kept constant for the lean and the rich gas mixture, respectively. The N_2O emission depends on the introduced reductant(s), and the nature of reductant acts differently depending on the temperature. At 200 °C, H_2 mainly drives the N_2O emission, whereas at 300 °C, N_2O yields is enhanced by C_3H_6 . In addition, it is demonstrated that NO_x reduction also occurs during the lean period, leading to significant amount of N_2O . In fact, on Pt–10% BaO/Al_2O_3 catalyst, 70–90% of the produced N_2O come from the lean phase, except with CO as reductant which does not allow any NO_x reduction in lean condition. Results were compared with a platinum/ceria–zirconia-based oxide (Pt/CZ) previously studied. Pt/CZ is generally more active at low temperature (200 °C). At 300 °C, significant differences appear between the two formulations depending on the used reductant, especially concerning the N-compound selectivities in the rich pulses.

© 2013 Elsevier B.V. All rights reserved.

1. Introduction

Catalytic elimination of environmental pollutants from passenger car is a permanent challenge for researchers. Particularly, NO_x reduction from exhaust gas of diesel and lean-burn engines is still a problem for car manufacturers. Among the processes effective to reduce NO_x in lean condition, two technologies are usually proposed: (i) the NO_x storage-reduction (NSR) concept [1,2], working in transient conditions; and (ii) the selective catalytic reduction (SCR). The SCR is described as a promising way to reduce NO_x , with the possible use of a large variety of reductants including unburned hydrocarbons, ammonia, urea, hydrogen or alcohol for instance. Actually, under the impulse of environmental legislation, the urea-SCR process is considered as a possible technological issue to reduce NO_x from light vehicles, as reported in numerous publications [1,3–11]. However, the NSR process has some interest since it does not require an additional reductant source. It works mainly in lean condition. NO_x are then oxidized on precious metals and stored on basic compounds, mainly as nitrates. Periodically, the catalyst is

submitted to rich conditions for a few seconds and the previously stored NO_x are reduced into N_2 on the precious metals. Among the disadvantages of this system, the selectivity of the reduction may be problematic. Indeed, an incomplete reduction leads to the formation of N_2O , a powerful greenhouse effect gas. The N_2O emission is usually observed at low temperatures (200–300 °C), whereas it tends to become zero at a higher temperature (400 °C). Another by product can also be observed when a high reduction level is achieved, namely NH_3 . Both N_2O and NH_3 emission during the NSR process must obviously be proscribed. However, ammonia produced during NSR cycles can be used in situ with the association of an adequate NH_3 -SCR catalyst [12]. NH_3 and N_2O can be observed during the NO_x reduction [13–19]. Ammonia formation is favored when H_2 is used as reductant, whereas CO is claimed to be the major responsible for N_2O emission [4,15,20].

Practically, the exhaust pipe usually contains a close-coupled catalyst which is placed in front of the NSR catalyst. This association is supposed to convert the three main pollutants, namely CO, unburned hydrocarbons (HC) and NO_x . However, due to the high cost of precious metals, this previous catalyst is not supposed to convert all CO and HC. A part of this job is dedicated to the NSR catalyst, which also contains precious metals. In another words, the global precious metal loading is partitioned between both

* Corresponding author. Tel.: +33 (0)549453994; fax: +33 (0)549453741.

E-mail address: xavier.courtois@univ-poitiers.fr (X. Courtois).

catalysts. As a consequence, untreated reductant can arrive on the NSR catalyst during the lean phases of the NSR process. Note that this precatalyst also strongly influences the composition of the rich mixture for the NO_x trap regeneration. Fuel is initially used as reductant, but it is partially transformed over the precatalyst and the NSR catalyst is finally submitted to a mixture of hydrocarbons, CO and H_2 with various compositions.

In a previous work, the NO_x conversion and selectivity over a ceria-zirconia-based oxide supported platinum NSR catalyst was studied using C_3H_6 , CO and H_2 as reductants, used separately or mixed [21]. Using complex gas mixtures including reductant(s) in both lean and rich media, it was showed that NO_x conversion and selectivity strongly depend on the used reductant and the temperature test. Especially, the contribution of the lean phase can largely contribute to the global N_2O formation, in accordance with the DeNO_x activity measurement in excess of oxygen.

In this work, the same scientific approach was applied to a usual 1%Pt–10%BaO/Al₂O₃ NSR model catalyst. The NO_x reduction efficiency was evaluated at 200, 300 and 400 °C with C_3H_6 , CO and H_2 as reductants, with a special consideration for the NO_x reduction selectivity.

These two platinum based catalysts exhibit very different redox behavior toward oxygen storage/mobility. The last part of this work puts in evidence the influence of the support formulation on the NO_x reduction behaviors.

2. Experimental

2.1. Catalyst preparation

10% BaO/Al₂O₃ material was prepared by the precipitation of barium salt ($\text{Ba}(\text{NO}_3)_2$) on alumina powder. First, the alumina was added in ultra-pure water and the temperature was raised at 60 °C. The pH was then increased to 10 by adding an ammonia solution, and the dry barium salt was added. After drying at 120 °C, support was calcined 700 °C for 4 h under air. After calcination at 700 °C, platinum (1 wt%) was impregnated using a $\text{Pt}(\text{NH}_3)_2(\text{NO}_2)_2$ aqueous solution. After drying, the catalyst was pre-treated at 700 °C for 4 h under N_2 , and finally stabilized at 700 °C for 4 h under a mixture containing 10% O_2 , 5% H_2O in N_2 . As previously reported [22], the intermediate nitrogen treatment allows higher platinum and barium dispersions. The obtained catalyst is denoted Pt–Ba/Al.

In this study, the Pt–Ba/Al behaviors are compared to another platinum based catalyst supported over a modified ceria-zirconia oxide provided by Rhodia and denoted Pt/CZ. The preparation and characterizations of Pt/CZ are detailed in Ref. [21]. Platinum (2.1 wt%) was added by impregnation. Catalyst was then calcined at 500 °C for 4 h under synthetic air and finally submitted to a hydrothermal treatment at 700 °C for 25 h.

2.2. Catalyst characterizations

The BET surface areas were deduced from N_2 adsorption at –196 °C carried out with a Micromeritics apparatus. Prior to the measurement, the samples were treated at 250 °C under vacuum for 8 h in order to eliminate the adsorbed species.

X-ray powder diffraction was performed at room temperature with a Bruker D5005 using a $\text{K}\alpha$ Cu radiation ($\lambda = 1.54056 \text{\AA}$). The powder was deposited on a silicon monocrystal sample holder. The crystalline phases were identified by comparison with the ICDD database files.

Platinum accessibility was determined with a Micromeritics AutoChem II instrument. Typically, 200 mg of sample were reduced in hydrogen flowing (30 mL min^{-1}) at 400 °C for 1 h, then

purged in ultrapure Ar (30 mL min^{-1}) for 2 h and cooled down to room temperature. Pulses of H_2 (0.5347 mL) were injected at –80 °C, every minute up to saturation (HC1). A new series of pulses was injected over the sample, after 10 min of purging under pure Ar, in order to determine the reversible part of the chemisorbed hydrogen (HC2). The irreversible part was taken as HC = HC1 – HC2.

The redox properties of catalysts were evaluated by temperature programmed reduction (TPR) experiments. Prior to the TPR test, the catalyst (100 mg) was first pretreated *in situ* under oxygen at 300 °C for 30 min and cooled to room temperature. After flushing under argon for 45 min, the reduction was carried out from room temperature up to 800 °C under a 1% H_2 /Ar mixture, using a $5 \text{ }^{\circ}\text{C min}^{-1}$ heating rate. The sample was maintained at 800 °C for 60 min before cooling under argon. Hydrogen consumption was followed by thermal conductivity.

Main characteristics of two studied catalysts are described thereafter. Pt–Ba/Al catalyst exhibits BET specific surface areas of $161 \text{ m}^2 \text{ g}^{-1}$ and a platinum dispersion of about 16% deduced from H_2 chemisorption measurements. XRD pattern of this sample (not shown) is consistent with previous reported analysis [22]. The main crystalline phase detected by XRD is BaAl₂O₄, and BaCO₃ is slightly evidenced. H₂-TPR measurement shows no significant hydrogen consumption, as previously reported for Pt–20%BaO/Al₂O₃ catalyst [23].

To compare, Pt/CZ material exhibits a BET specific surface area of $82 \text{ m}^2 \text{ g}^{-1}$. The platinum dispersion was measured at 16%, as for Pt–Ba/Al. XRD analysis showed only one crystallized structure corresponding to a solid solution with a ceria cubic fluorite-like structure. The H₂-TPR characterization (not shown) evidenced a high reducibility, with a main reduction peak at around 150 °C. It corresponds to both the platinum reduction and the easily reducible Ce^{IV} reduction in Ce^{III}. The related H₂ consumption reaches $557 \mu\text{mol H}_2/\text{g}_{\text{cata}}$, whereas the total H₂ consumption in the 25–800 °C temperature range is $938 \mu\text{mol H}_2/\text{g}_{\text{cata}}$.

2.3. NO_x storage capacity (NSC) measurement

Before measurements, the catalyst (70 mg) was firstly pre-treated *in situ* for 15 min at 500 °C, under a 10% O_2 , 10% H_2O , 10% CO_2 and N_2 mixture, and then cooled down to 400 °C with the same mixture. The catalyst was then submitted to a reducing treatment (4% CO, 1.33% H_2 , 10% H_2O , 10% CO_2 and N_2) for 15 min and cool down to 200 °C under the same mixture. After a purge under N_2 , the sample was then submitted to 500 ppm NO, 10% O_2 , 10% H_2O , 10% CO_2 and N_2 mixture. For measurements at 300 °C and 400 °C, the catalyst is treated in reducing mixture during the increase of the temperature. The total flow for the whole procedure is constant at 20 L h^{-1} . It corresponds to a gas hour space velocity (GHSV) of about $200,000 \text{ h}^{-1}$ for Pt–Ba/Al catalyst. It is a little higher with Pt/CZ since its apparent density is higher. The gas flow was introduced using mass-flow controllers, except for H_2O which was introduced using a saturator. Gas analysis (NO, NO_2) was performed by a Multigas MKS 2030 analyzer (FTIR). Long time storage is not representative of the NSR catalyst working conditions, since the lean periods are commonly around 1 min. The NO_x storage capacity was then estimated by the integration of the recorded profile for the first 60 s, equal to the lean periods of the NSR test in cycling conditions (see below). The contribution of the reactor volume was subtracted. With the conditions used in this test, $99.2 \mu\text{mol NO}_x$ per gram of catalyst were injected in 60 s. Then, the NO_x storage capacity for 60 s expressed in $\mu\text{mol NO}_x/\text{g}$ almost corresponds to the storage rate (%).

In addition, the platinum oxidation activity was estimated as the NO_2/NO_x ratio (%) at saturation (usually after about 900 s).

Table 1

Rich and lean gas compositions used for the NO_x conversion test (60 s lean/4 s rich). Total flow rate: 20 L h⁻¹ (GHSV = 200,000 h⁻¹). The redox ratio is constant at 0.017 at 3.35 with lean and rich gas mixture, respectively.

| Gas | | Reducant | | | Oxidant | | Common gases | | |
|---|----------|-------------------------------|----------|----------------|---------|----------------|-----------------|------------------|----------------|
| | | C ₃ H ₆ | CO | H ₂ | NO | O ₂ | CO ₂ | H ₂ O | N ₂ |
| Full gas | Lean (L) | 300 ppm | 500 ppm | 167 ppm | 500 ppm | 10% | 10% | 10% | Balance |
| | Rich (R) | 9000 ppm | 4% | 1.33% | 100 ppm | 2% | | | |
| Only C ₃ H ₆ as reductant | Lean (L) | 374 ppm | – | – | 500 ppm | 10% | 10% | 10% | Balance |
| | Rich (R) | 1.49% | – | – | 100 ppm | 2% | | | |
| Only CO as reductant | Lean (L) | – | 3300 ppm | – | 500 ppm | 10% | 10% | 10% | Balance |
| | Rich (R) | – | 13.4% | – | 100 ppm | 2% | | | |
| Only H ₂ as reductant | Lean (L) | – | – | 3300 ppm | 500 ppm | 10% | 10% | 10% | Balance |
| | Rich (R) | – | – | 13.4% | 100 ppm | 2% | | | |

2.4. NO_x conversion in cycling conditions

Before measurements, the catalyst (70 mg) was treated in situ 15 min at 500 °C under the full gas lean mixture, displayed in Table 1. The sample was then cooled down to 200 °C under the same mixture. The NO_x conversion was studied in cycling condition by alternatively switching between lean (60 s) and rich (4 s) conditions using electro-valves. The lean and rich gas compositions are described in Table 1. Most gases (NO, NO₂, N₂O, NH₃, CO, CO₂, C₃H₆...) were analyzed using a Multigas FTIR detector (MKS 2030), except H₂ which was analyzed by mass spectrometry. NO_x reduction into N₂ is calculated assuming no other N-compounds than NO, NO₂, N₂O and NH₃, neither HNCO which was never detected. For each tested temperature (200, 300 and 400 °C), the activity of the catalyst was followed until stabilization and calculations were done taking into account ten cycles after stabilization.

Supplementary tests were carried out with simplified gas mixtures, i.e. with only one reducing compound (C₃H₆ or CO or H₂), but with the same reductant/oxidant ratio as used with the full gas mixture (Table 1). The reductant/oxidant ratio (i.e. the redox stoichiometry of the gas mixture) is calculated using Eq. (1), and corresponds to 0.017 and 3.35 for the lean and the rich gas mixture, respectively.

$$\text{red/ox} = \left(\frac{9 \times [\text{C}_3\text{H}_6] + [\text{CO}] + [\text{H}_2]}{[\text{NO}] + 2[\text{O}_2]} \right) \quad (1)$$

2.5. Light-off tests in lean mixture

The lean DeNO_x behaviors of the catalysts were also examined using only the lean mixtures reported in Table 1. Before measurement, catalyst (70 mg) was treated in situ 15 min at 500 °C under the chosen lean mixture. The N-compounds concentration (NO_x, N₂O, NH₃) were recorded from 500 °C down to 200 °C under the same mixture.

3. Results

In this part is depicted the catalytic properties of the Pt–Ba/Al NSR model catalyst depending on the operating conditions.

3.1. NO_x storage capacities (NSC)

In order to have a good understanding of the NO_x reduction efficiency in cycling condition, the NO_x storage capacity of Pt–Ba/Al was evaluated at 200, 300 and 400 °C using the lean mixture of the NSR test, but without any reductant in the feed stream. The amount of stored NO_x for 60 s (μmol/g), length of the lean periods for the NSR test, is reported in Table 2. It increases with temperature, from 9 to 46 μmol/g at 200 °C and 400 °C, respectively. In parallel, the NO oxidation rate, estimated by the NO₂/NO_x ratio after saturation,

Table 2

NO_x storage capacity (μmol/g) for 60 s (NO_x storage fraction; inlet: 500 ppm NO, 10% O₂, 10% H₂O, 10% CO₂ and N₂, 200 mL min⁻¹) and NO₂/NO_x ratio after saturation for Pt–Ba/Al catalyst.

| Temperature test | 200 °C | 300 °C | 400 °C |
|---|--------|--------|--------|
| NO _x storage capacity (μmol/g) | 9 | 22 | 46 |
| NO ₂ /NO _x (%) | 14 | 57 | 60 |

also increases with the temperature (Table 2), with a maximum of 60% obtained at 400 °C, which is very close to the thermodynamic equilibrium.

Since the NO_x storage capacity for the first 60 s almost corresponds to the NO_x storage rate (%), it appears that it is rather limited. This behavior is mainly attributed to the presence of H₂O and CO₂ in the gas mixture [24]. Water affects the oxidation activity of the catalysts, leading to a decrease of NO oxidation activity of Pt, while CO₂ competes with NO_x for the adsorption on the basic storage sites. The more the basic strength of the storage sites is high, the more the carbon dioxide competes [24].

3.2. NSR efficiency

Catalytic results of NSR experiments in cycling conditions are presented in Fig. 1, for the full gas mixture depicted in Table 1, including reductants in both lean and rich mixtures. Such complex

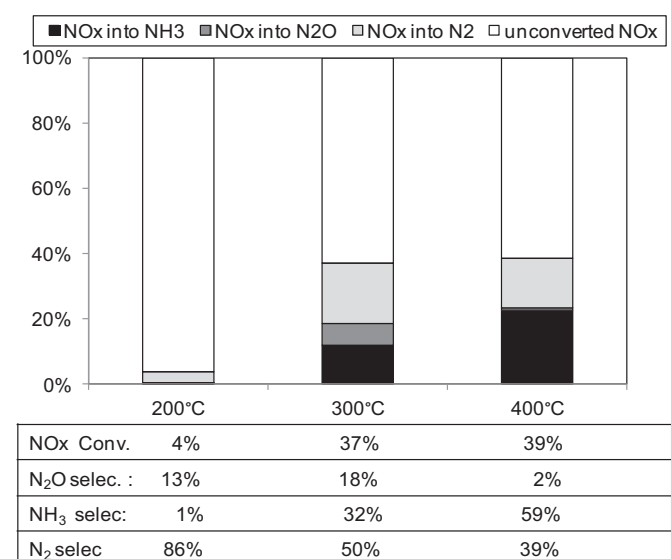


Fig. 1. NO_x storage/reduction efficiency test at 200, 300 and 400 °C (full gas) over Pt–Ba/Al catalyst.

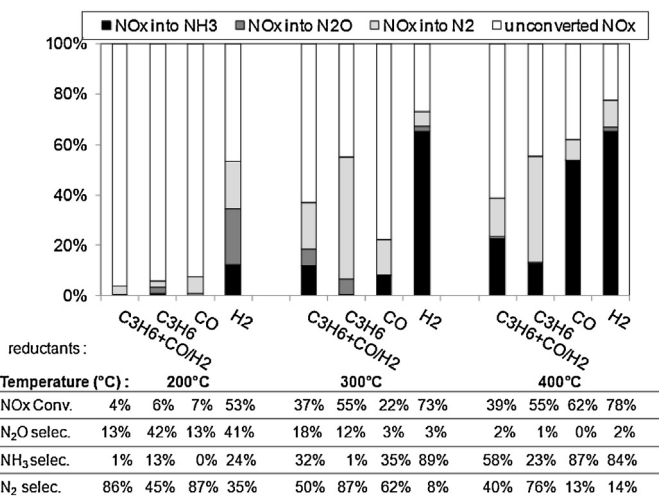


Fig. 2. Effect of the nature of the reductant(s) (in both lean and rich gas mixture) on NO_x storage/reduction efficiency and selectivity at 200 °C, 300 °C and 400 °C over Pt–Ba/Al catalyst.

conditions are usually not applied in literature and infer some new results.

Firstly, NO_x conversions reported in Fig. 1 are lower than corresponding NO_x storage capacity, indicating that the reduction of the stored NO_x is the limiting step, as already reported in previous work with simplified gas mixture and higher barium loading (1%Pt/20%BaO/Al₂O₃ sample) [25]. As expected, Fig. 1 shows that both NO_x conversion and selectivity depend on the temperature test. At 200 °C, with the whole of reductants, the NO_x conversion is very low (4%). It increases to 37% at 300 °C and reaches 39% at 400 °C.

Concerning the selectivity, both N₂O and NH₃ undesired by-products are emitted. The best N₂ selectivity is obtained at 200 °C (86%), but it is not very significant since the NO_x conversion is very low at this temperature. For higher temperatures and conversions, the NH₃ selectivity increases from 32% at 300 °C to 59% at 400 °C. On the opposite, N₂O selectivity strongly decreases with the temperature, from 18% at 300 °C to 2% at 400 °C. Finally, the nitrogen selectivity reaches only 50% at 300 °C, and 39% at 400 °C.

In the next part of this work, the NO_x storage-reduction efficiency was evaluated depending on the nature of the reductant.

3.3. Influence of the nature of the reductant on the NO_x conversion and selectivity

The effect of various reducing agent (H₂, CO, C₃H₆) on the efficiency and selectivity of NSR catalysts was already studied on platinum supported on alumina-based oxides [15,26,27], but usually with simplified mixtures. Using CO or C₃H₆ as reducing agents, authors have reported that significant N₂O emission occurs rather at low temperature (i.e. $T \leq 300$ °C). Lindholm et al. [28] have also reported that N₂O formation can be observed with H₂, depending on the hydrogen concentration: the higher is the H₂ concentration, the higher is the N₂O formation.

In this part of the study, the NO_x conversion and selectivity over the Pt–Ba/Al catalyst was investigated using only one reductant (the same) in both lean and rich gas mixtures, with compositions reported in Table 1. Results are presented in Fig. 2. Results with the whole reductants (C₃H₆ + CO + H₂) were also reported for comparison.

At 200 °C, using only C₃H₆ or CO as reductant, the NO_x conversion remains low (<7%), as with the mix of the three reductants. Compared with the full gas, the N₂O selectivity is not affected using

only CO, at 13%, but it significantly increases to 42% when only propylene is introduced. The NO_x conversion strongly increases with H₂ as single reductant, up to 53%. These results illustrate the competitive adsorptions between each reductant when they are blended together at 200 °C. With H₂, the N₂O selectivity reaches a value close to the one observed with C₃H₆, at 41%. In the same time, high ammonia yield is also observed at 24%. As a consequence, the nitrogen selectivity reaches only 35% at 200 °C.

At 300 °C, various results are also obtained depending on the nature of the reductant(s) (Fig. 2). Compare with tests obtained with the “full gas” mixture, NO_x conversion is enhanced with only C₃H₆ or H₂, at 55% and 73%, respectively. On the contrary, using CO as reductant leads to the lower NO_x conversion at this temperature at only 22%. This result appears surprising since NSR experiments performed at 400 °C show a higher NO_x conversion with CO than with the “full gas” mixture. This point is discussed in Section 3.4.

Selectivities also strongly differ. Using propylene as single reductant leads to a N₂O selectivity of 12%, which is quite close to the one obtained with the mixture of the three reductants (18%). On the contrary, low N₂O selectivity is observed with CO or H₂ as reductant (3%).

Concerning ammonia, it is almost not emitted with propylene whereas the NH₃ selectivity reaches 89% with H₂. Note that the presented result is obtained using a very high H₂ concentration in the rich pulses (13.4%), in order to respect the fixed reductant/oxidant ratio (Table 1). Then, this behavior is in accordance with literature which reports that NH₃ formation is favored in case of unconverted hydrogen [25]. With only CO, NH₃ selectivity is 35%, close to the one observed with the full gas, which is quite surprising. The ammonia formation mechanism was largely studied in the literature. Ammonia can be formed via the isocyanate route when CO is used as the main reductant, as reported in [29,30]. NH₃ can also be formed by the direct reaction of H₂ with NO_x [31,16]. Besides, due to water gas shift equilibrium reaction (CO + H₂O ⇌ CO₂ + H₂) H₂ can be produced even if only CO is introduced. This point is discussed in Section 4.2.

Results obtained at 400 °C show that the NO_x conversions are quite similar to those measured at 300 °C, except using only CO as previously mentioned. The N₂O selectivity tends to be nil at this temperature. On the contrary, the ammonia selectivity becomes very high, at around 85% using H₂ or CO, and 58% with the complete reducing mixture. Propylene still allows the lower ammonia selectivity, at 23%.

To conclude, NO_x conversion and N-compound selectivities depends on the temperature and reductants. At low temperature (200 °C), H₂ is the only significantly effective reductant, but N₂O is the main product. At 300 °C, H₂ or C₃H₆, considered separately, enhance the NO_x efficiency. Propylene leads to an important formation of N₂O whereas H₂ strongly favors NH₃. For higher temperature (400 °C), N₂O tends to be nil whatever the used reductant(s), but NH₃ becomes the main product, excepted with C₃H₆ as reductant.

Considering that ammonia is an interesting NO_x reductant, especially in lean atmosphere, N₂O appears the more problematic by-product of the NO_x reduction. The next parts of this work focus on the influence of the nature of the reductant agent on the N₂O emission.

3.4. Influence of reductant(s) in the lean phases on the N₂O formation

It is generally admitted that the N₂O formation over precious metals comes from the recombination of atomic N (from the NO dissociative adsorption on metallic platinum sites) with adsorbed NO [32]. In NSR cycles, N₂O was reported to be especially detected during the lean/rich switches, due to a lack in metal reduction [27]. Results reported above in this study show that the

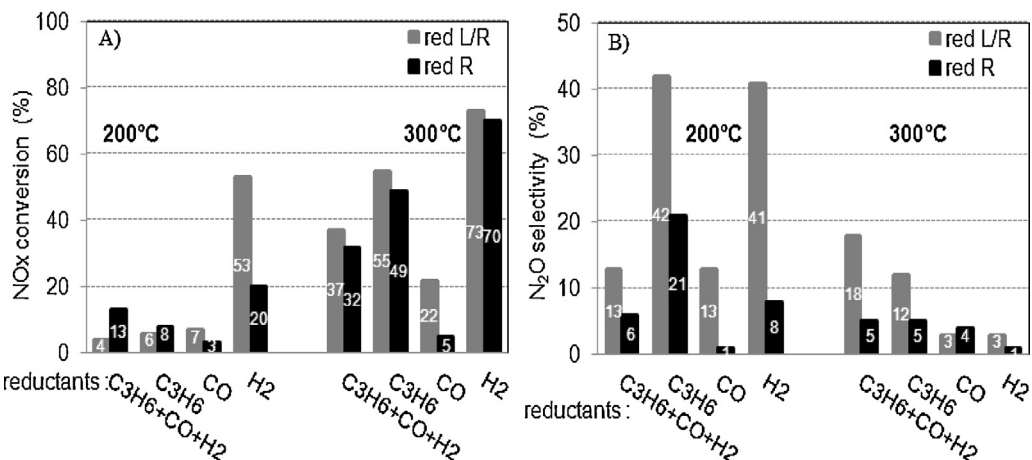


Fig. 3. Influence of the absence of reductant(s) in the lean mixture at 200 °C and 300 °C over Pt–Ba/Al catalyst on (A) NO_x conversion and (B) N₂O selectivity. Results in gray (red L/R) correspond to test with reductant(s) in both lean and rich mixtures; results in black (red R) correspond to test with reductant(s) only in rich mixtures.

composition of the rich and lean gas mixtures dramatically modifies the catalytic results. Particularly, compared with simplified NSR experiments usually reported in literature (i.e. without reductant(s) during the lean storage phases for instance), high N₂O selectivities are observed. Then, in order to evaluate the contribution of each lean and rich phase on the N₂O emission, operating conditions were modified.

3.4.1. Tests without reductants in the lean mixture

With the aim to obtain more information about the N₂O production, new catalytic tests were performed without reductants in the lean mixture (flow rate was kept constant by adding N₂). The temperatures of 200 and 300 °C were selected since no significant amount of N₂O is emitted at 400 °C. The influence of the absence of reductant(s) in the lean mixtures is depicted in Fig. 3.

Firstly, at 200 °C, it appears from Fig. 3A that the absence of reductant in the lean mixture leads to increase the NO_x conversion for tests carried out with C₃H₆ (C₃H₆ + CO + H₂ reducing mixture or C₃H₆ alone). This improvement is particularly significant considering the mix of reductants (C₃H₆ + CO + H₂), the NO_x conversion growths from 4% to 13% when reductants are removed from the lean mixture. This observation is attributed to an inhibiting effect of C₃H₆ on the NO oxidation on platinum during the lean periods: using the full gas mixtures, only few ppm of NO₂ are detected (all produced NO₂ are trapped), whereas an average value of 145 ppm NO₂ is recorded when C₃H₆ is removed from the lean mixture (recorded profiles not shown). Different results are obtained with CO or H₂ as reductant since the NO_x conversion decreases of about 50% if CO or H₂ is removed from the lean mixture. These decreases are associated with remarkable drops in N₂O selectivity (Fig. 3B). It tends to be nil when CO is suppressed from the lean mixture, and a drop of about 80% is observed for hydrogen. Same trends are also observed from tests with propylene (C₃H₆ alone or mixed with CO and H₂), the N₂O selectivity is divided by two.

At 300 °C, as depicted above, higher NO_x conversions are obtained compared to tests at 200 °C. Tests carried out with C₃H₆ (alone or mixed with CO and H₂) show that the NO_x conversion slightly decreases when reductant is removed from the lean mixture. In the same time, the N₂O selectivity is strongly altered, by a factor 2.4 to 3.6. Same trends are observed considering H₂ as reductant, but, as already mentioned, the obtained N₂O selectivity is low at this temperature. Results are more complex with CO. A decrease of 77% of the NO_x conversion is observed when CO is removed from the lean mixture (Fig. 3A). This surprising result is illustrated in Fig. 4 by the NO_x and CO concentration profiles recorded during the

NSR experiments, with or without CO in the lean mixture. Note that the rich pulses appear longer than 4 s due to the gas dilution mainly due to the volume of the IR cell. It is observed that CO conversion is higher in the rich pulses when carbon monoxide is present in both lean and rich mixture (full line). On the opposite, similar CO concentration profiles are obtained during the lean periods even if CO is introduced in the lean mixture (same observed minima). This result indicates a total CO conversion in lean atmosphere. In parallel, NO_x storage fraction is higher when CO is present in the lean period, but a strong increase in NO_x concentration is also observed when switching to rich atmosphere, indicating an important NO_x desorption. In fact, it corresponds to NO emission (NO concentration profiles not shown). Then, it clearly appears that CO in lean mixture favors the NO_x reduction during the rich pulses, while the N₂O selectivity is not affected (Fig. 3B). Furthermore, as presented in the next section, CO does not allow any significant NO_x reduction in lean mixture (Fig. 6D), but it is fully converted into CO₂. In addition, it is assumed that the NO_x reduction during the rich phases occurs over reduced metallic sites, which are needed to allow the NO_x dissociative adsorption. As a consequence, we suppose that CO oxidation in the lean phase modifies the platinum redox state since CO removes the adsorbed oxygen atoms (Pt–O_a) from the Pt particles to form CO₂, leading to the regeneration of the metallic platinum sites [29]. It would lead to an easier platinum reduction

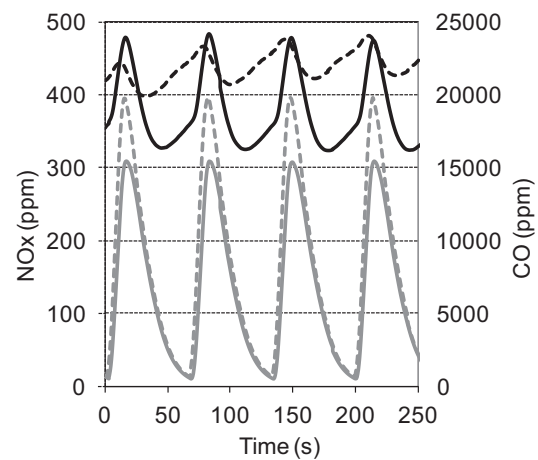


Fig. 4. NSR cycles at 300 °C over Pt–Ba/Al catalyst using CO as reductant: comparison of NO_x (—, ---) and CO (—, ---) outlet profiles with (full lines) or without (dotted lines) CO in lean mixture.

at the beginning of the rich pulses. At 400 °C, the catalyst reduction during the rich pulses is faster, the NO_x conversion strongly increases (Fig. 2) and there is no more influence of the presence of CO in the lean mixture (result not shown).

The N₂O profiles recorded during the NSR cycles at 300 °C are detailed in Fig. 5 depending on the presence or absence of reductant in the lean mixture. As expected, Fig. 5B shows that N₂O is not produced during the lean periods if there is no reductant in the lean mixture. On the contrary, significant N₂O concentrations are detected if reductants are added in the lean mixture (Fig. 5A). In accordance with results reported in Fig. 3B, it appears that N₂O is largely detected during the lean phases when C₃H₆ is used (alone or mixed with CO and H₂). Few ppm of N₂O are also detected using H₂, whereas near no N₂O emission is observed during the lean phases with CO as reductant.

3.4.2. Light-off tests in lean mixture

In order to have a better overview of the N₂O formation during the lean steps of the NSR process depending of the temperature, new experiments were performed in light-off mode with conditions corresponding to usual SCR experiments in lean condition, using the different lean mixtures reported in Table 1. Results reported in Fig. 6 show the NO_x and N₂O concentrations profiles recorded in the 200–400 °C temperature range. As previously suggested, near no NO_x reduction is observed with CO as reductant (Fig. 6D), with a maximum of 2–3 ppm of N₂O emitted. Nevertheless, CO is fully oxidized into CO₂ in the whole 200–400 °C temperature range. The NO_x conversion in excess of oxygen can be effective with other reductants over Pt–Ba/Al, but it depends on the temperature and the nature of reductant. With the whole reductants (C₃H₆ + CO + H₂, Fig. 6A), the NO_x conversion is low at 200 °C, with 2 ppm of N₂O emitted. The NO_x conversion reaches a maximum of about 20% at 220 °C, corresponding to a N₂O emission of 40 ppm (black full line, Fig. 6A). Increasing the temperature leads to the decrease of the NO_x conversion to 10% at 300 °C, with a corresponding N₂O emission of 11 ppm. No more NO_x conversion is observed at 400 °C. Interestingly, similar profiles are obtained with propylene as single reductant (Fig. 6B). The maximum NO_x conversion (about 22%) is obtained at 230 °C and 49 ppm of N₂O are emitted. At 300 °C, the N₂O concentration reaches 13 ppm, and it tends to zero at 400 °C. From these results it appears that N₂O emission is enhanced with propylene as only reductant, but in order to keep the same oxidant/reductant ratio, a higher C₃H₆ concentration was used compared to the full gas (Table 1). The obtained NO_x profiles are consistent with those reported in literature for NO_x SCR by hydrocarbons over platinum based catalysts [33–37], with maximum NO_x conversion between 200 and 300 °C and a high N₂O selectivity at low temperature.

NO_x conversion is also effective with H₂ as reductant, but mainly for lower temperatures (Fig. 6C), in accordance with other reported studies over platinum based catalysts [38,39].

The maximum NO_x conversion is obtained at 200 °C (19%), with the formation of about 17 ppm of N₂O. Then, both NO_x conversion and N₂O concentration significantly decrease with temperature, they are nil at 300 °C. Finally, note that ammonia emission is never observed in lean condition.

Results reported in this section show good agreements between tests carried out in lean mixture (light-off test) and N₂O values recorded at the end of the lean periods during the NSR tests at 200 and 300 °C. Major difference is observed for tests performed with hydrogen at 300 °C. There is no N₂O emission detected when the test is carried out exclusively in lean mixture, whereas 3.4 ppm of H₂ are recorded at the end of the lean periods during the NSR tests. In order to clarify this point, tests with gas dilution after the reactor were performed to allow a faster purge of the IR cell. Obtained results were then consistent with those recorded at the end of the

lean period, taking into accounts that the gas dilution (by a factor 5) induced also a loss of sensibility.

To conclude about the N₂O emission during the lean periods due to the presence of reductant(s), it appears that at 200 °C, N₂O emission is essentially favored when H₂ is used as only reductant. At higher temperature, N₂O emission is mainly related to the presence of C₃H₆, with a maximum N₂O emission near 220–230 °C. CO is nearly inactive toward NO_x reduction in the whole studies temperature range.

3.5. Contribution each lean and rich phase on the N₂O formation

Based on results reported in the previous section, the distribution of the N₂O formation during each lean and rich phase of the NSR cycles has been evaluated. For the lean periods, we have selected the last N₂O concentration recorded before the switch to the rich mixture. Integration of the N₂O peak associated with the rich phase was used to obtain an average value for the length of the rich pulse (4 s). Results are reported in Table 3, associated with the NO_x conversion and the N₂O selectivity.

At 200 °C, the NO_x conversions are too low to be discussed toward N₂O distribution, except with H₂ as single reductant. In this case, NO_x conversion and N₂O selectivity reach 53% and 41%, respectively. Calculations from recorded N₂O profile show that 91% of nitrous oxide is emitted during the lean period, due to the significant NO_x reduction in excess of O₂ at low temperature (Fig. 6C).

At 300 °C, N₂O yields of approximately 7% are obtained using the full gas mixture (C₃H₆ + CO + H₂) or only propylene. Again, the major part (71–72%) of the N₂O emission is attributed to the lean phases. This is also the case using only H₂ as reductant (66%), but the N₂O selectivity is then low, at 3%. Finally, only CO, which is not really active in NO_x reduction in excess of oxygen over Pt–Ba/Al, leads a major contribution of the rich pulses on the N₂O formation, but the global N₂O concentration is recorded at a low level.

4. Influence of the redox behavior of the support: Pt–Ba/Al versus Pt/CZ

In a previous work [21], with the same approach as described above, the NO_x conversion and selectivity were discussed toward platinum supported over a ceria–zirconia-based oxide catalyst (Pt/CZ), with a special attention to the N₂O formation during the NSR process. Even if platinum loading, NO_x storage component and specific surface area differ for both Pt–Ba/Al and Pt/CZ catalysts, the main difference between both catalysts is their respective redox properties. Barium–alumina supports exhibits no significant redox behavior, whereas Pt/CZ is reducible by a large extend. Comparison of the catalytic behaviors of these catalysts is depicted below.

4.1. NO_x conversion and NO_x reduction selectivity in cycled condition

At 200 °C, as previously described (Fig. 2), the NO_x conversion over Pt–Ba/Al catalyst is significantly effective only with H₂ as reductant. The NH₃ and N₂O selectivity reach 24% and 41%, respectively, and more than 90% of the emitted N₂O is produced during the rich pulses. Compared to Pt–Ba/Al, Pt/CZ catalyst is more active at this temperature, and significant NO_x reductions are observed whatever the considered reductant (Table 3). Using H₂, the NO_x conversion reaches 92%. The ammonia selectivity is limited at 2% [21]. Interestingly, N₂O selectivity (43%) and the N₂O distribution (78% from the lean phases) are very similar than those calculated for Pt–Ba/Al. Other results obtained at 200 °C over Pt/CZ with other reducing mixtures are discussed in [21]. However, note that the higher N₂O selectivities (47–62%) are observed with C₃H₆ (alone or mixed with CO and H₂), with a main contribution of the lean periods

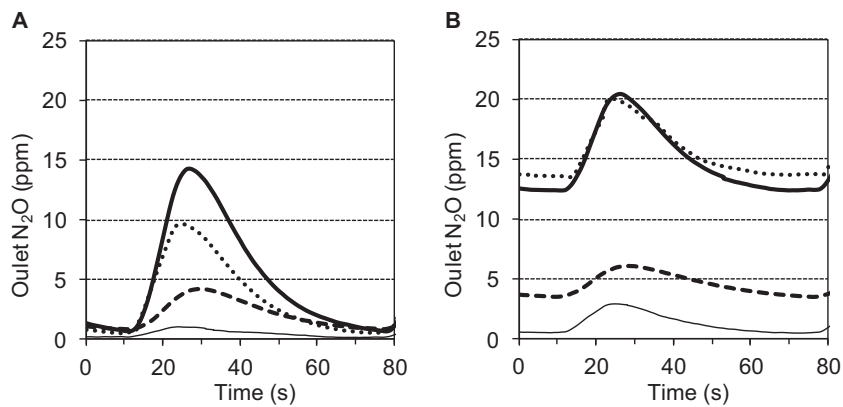


Fig. 5. N₂O profiles recorded during NSR cycles at 300 °C over Pt–Ba/Al catalyst depending on the used reductant(s): C₃H₆ + CO + H₂ (···); C₃H₆ (—); CO (—) or H₂ (---). Reductant(s) present in lean and rich mixtures (A) or only in the rich pulses (B).

(78% of the emitted N₂O using C₃H₆, and 61% using C₃H₆ + CO + H₂, Table 3). On the opposite, the N₂O selectivity is limited at 20% using CO, and most of the N₂O emission (87%) occurs during the rich pulses.

At 300 °C, comparison of NO_x conversion and selectivity over both Pt–Ba/Al and Pt/CZ is illustrated Fig. 7, depending on the introduced reductant(s) in both lean and rich mixtures of the NSR test. It clearly appears that the NO_x conversion is more sensitive to the nature of the introduced reductant over Pt–Ba/Al than over Pt/CZ, with conversion ranges of 22–73% and 49–64%, respectively. Besides, Fig. 7 also highlights a strong influence of the support composition on the ammonia selectivity at 300 °C. It does not exceed 7% on Pt/CZ catalyst whatever the considered reductant(s), whereas NH₃ emissions can be very high on Pt–Ba/Al catalyst, especially

using hydrogen as reductant (NH₃ yield = 65%, S_{NH₃} = 89%). In fact, the selective NH₃ oxidation into N₂ was previously proposed for platinum supported over reducible oxide to explain the low ammonia emission in NSR test using H₂ as reductant [40]. Only the use of propylene as single reductant leads to similar NO_x conversions (52–55%) and low ammonia selectivities (1%) for both catalysts. At 300 °C, Fig. 7 also shows that the global N₂O selectivity is lower on Pt–Ba/Al than on Pt/CZ, whatever the reductant(s). However, the same evolutions are observed depending on the reducing agent. The higher N₂O selectivities are obtained using the full reducing mixture (C₃H₆ + CO + H₂) or only propylene, with values of 18% and 12% for the Pt–Ba/Al, versus 22% and 20% on Pt/CZ sample. The N₂O selectivities drop to 3% with CO or H₂ as reductant using the Pt–Ba/Al catalyst, and to 10% and 5% with Pt/CZ, respectively. A

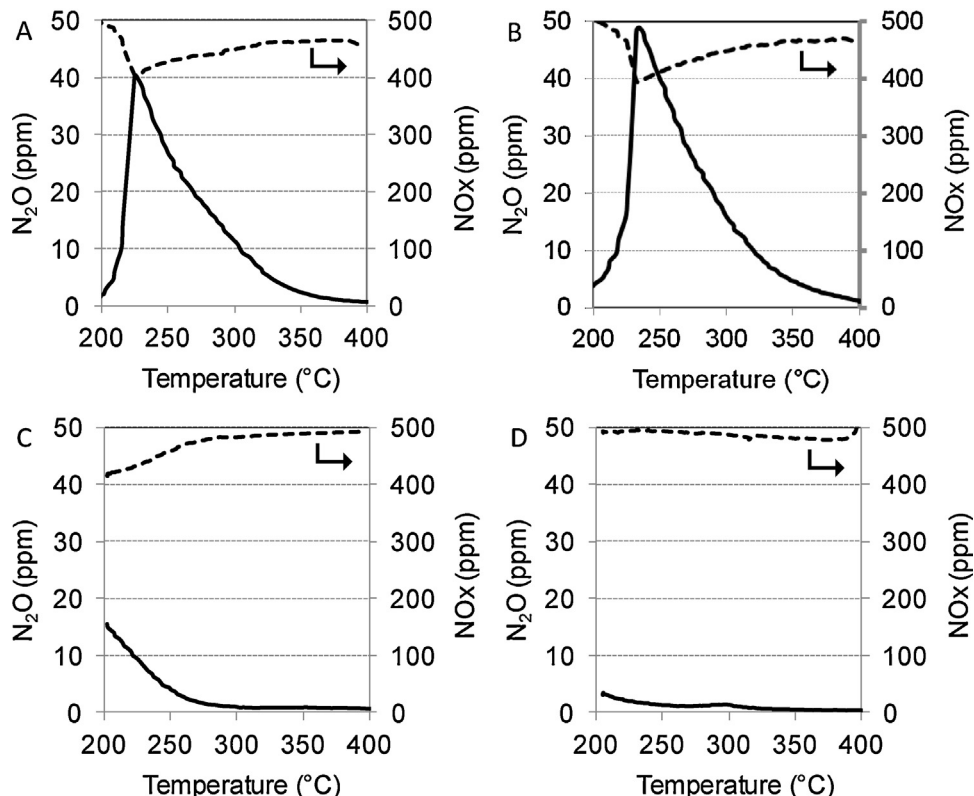


Fig. 6. Catalytic tests over Pt–Ba/Al catalyst in lean mixture depending on the introduced reductant(s): NO_x concentration (dotted line) and N₂O concentration (full line). (A) 500 ppm NO + 10% O₂ + (300 ppm C₃H₆ + 500 ppm CO + 167 ppm H₂). (B) 500 ppm NO + 10% O₂ + 374 ppm C₃H₆). (C) 500 ppm NO + 10% O₂ + (3300 ppm H₂). (D) 500 ppm NO + 10% O₂ + (3300 ppm CO).

Table 3

NO_x conversion, N_2O selectivity and N_2O distribution between lean and rich mixtures of the NSR cycles (and corresponding average of N_2O concentration) at 200 °C and 300 °C for Pt–Ba/Al and Pt/CZ catalysts.

| | 200 °C | | | | 300 °C | | | |
|---|---------------------|--------------------------|-----------------------------------|--------------|---------------------|--------------------------|-----------------------------------|--------------|
| | Cycled tests | | N_2O distribution | | Cycled tests | | N_2O distribution | |
| | NO_x conv. | $S_{\text{N}_2\text{O}}$ | Lean | Rich | NO_x conv. | $S_{\text{N}_2\text{O}}$ | Lean | Rich |
| Pt–Ba/Al | | | | | | | | |
| $\text{C}_3\text{H}_6 + \text{CO} + \text{H}_2$ | 4% | 13% | 37% 0.4 ppm | 63% 0.8 ppm | 37% | 18% | 72% 11.4 ppm | 28% 4.4 ppm |
| C_3H_6 | 6% | 42% | 78% 4.6 ppm | 22% 1.3 ppm | 55% | 12% | 71% 11.2 ppm | 29% 4.6 ppm |
| CO | 7% | 13% | 67% 1.4 ppm | 33% 0.7 ppm | 22% | 3% | 32% 0.5 ppm | 68% 1.1 ppm |
| H_2 | 53% | 41% | 91% 47.3 ppm | 9% 4.7 ppm | 73% | 3% | 66% 3.4 ppm | 34% 1.8 ppm |
| Pt/CZ | | | | | | | | |
| $\text{C}_3\text{H}_6 + \text{CO} + \text{H}_2$ | 40% | 47% | 61% 27.8 ppm | 39% 17.8 ppm | 49% | 22% | 45% 11.2 ppm | 55% 14.4 ppm |
| C_3H_6 | 15% | 62% | 78% 17.2 ppm | 22% 4.9 ppm | 52% | 20% | 45% 11.3 ppm | 55% 13.8 ppm |
| CO | 58% | 20% | 13% 3.6 ppm | 87% 24.5 ppm | 56% | 10% | 10% 1.3 ppm | 90% 12.2 ppm |
| H_2 | 92% | 43% | 78% 74.9 ppm | 22% 21.1 ppm | 64% | 5% | 60% 4.7 ppm | 40% 3.1 ppm |

detailed comparison of the N_2O emissions during the lean and rich periods is reported in Section 4.3.

In order to understand these different behaviors in NO_x conversion for Pt–Ba/Al and Pt/CZ, the possible transformation of the introduced reductant during the rich pulse was envisaged since the reaction mixture included 10% H_2O and 10% CO_2 . Indeed, ceria-based catalyst are known to enhance the water–gas-shift (WGS) reaction [41]. A comparison of the behaviors of both Pt–Ba/Al and Pt/CZ catalyst in reductant transformation is detailed thereafter in Section 4.2.

4.2. Reductants transformation during the rich pulses

The possible reductants transformation was examined by comparing the reductants profiles recorded in by-pass to profiles recorded during the tests. Note that this procedure does not allow to access to the real amount of transformed reductant since a part of reductants reacts during the test. For both the Pt–Ba/Al and Pt/CZ catalysts, the CO, H_2 or C_3H_6 transformation in the rich pulses was examined at 200 °C and 300 °C and results are reported in Figs. 8–10, respectively.

When CO is the only reducing agent in the rich pulses, results presented in Fig. 8 show that no H_2 emission is detected at 200 °C with Pt–Ba/Al, whereas H_2 is emitted in high amount over Pt/CZ

(maximum concentration: 1.78%). At 300 °C, pulses of H_2 are then detected during the CO rich pulses over Pt/Ba–Al, with a maximum H_2 concentration recorded at 486 ppm, while maxima of 2.37% are detected with Pt/CZ. These results demonstrate the higher activity of Pt/CZ catalysts for the water gas shift (WGS) reaction ($\text{CO} + \text{H}_2\text{O} \rightleftharpoons \text{CO}_2 + \text{H}_2$).

With H_2 as reductant in the rich pulses, Fig. 9 illustrates that significant CO emission is detected from 200 °C, whatever the catalyst formulation. However, Pt/CZ sample clearly enhances the CO formation by the reverse water gas shift (RWGS) reaction ($\text{CO}_2 + \text{H}_2 \rightleftharpoons \text{CO} + \text{H}_2\text{O}$). At 200 °C, the maximum CO concentrations are 82 ppm and 325 ppm for Pt–Ba/Al and Pt/CZ catalyst, respectively. At 300 °C, these concentrations increase to 229 ppm and 503 ppm, respectively. Then, even if only H_2 is introduced, both H_2 and CO are detected at 200 °C and 300 °C, but CO emission is higher on the catalyst supported over the reducible support.

Tests with C_3H_6 as inlet reductant also show some possible transformation. Few ppm CO are detected at 200 °C and 300 °C over Pt–Ba/Al. Same results are obtained with Pt/CZ at 200 °C, but more significant transformation is evidenced 300 °C. Indeed, peaks of H_2 , CO and CH_4 are detected with maximum concentrations of 1.47%, 435 ppm and 250 ppm, respectively (Fig. 10). From these observations, it is assumed that steam reforming of C_3H_6 occurs on Pt/CZ at 300 °C.

Note that for Pt–Ba/Al, all these results are in perfect accordance with results previously established about the ammonia emission [25,42]. Using simplified gas mixtures (lean: $\text{NO} + \text{O}_2 + \text{CO}_2 + \text{H}_2\text{O}$ in N_2 ; rich: $\text{H}_2 + \text{CO}_2 + \text{H}_2\text{O}$ in N_2), it was demonstrated that ammonia is detected in the outlet gas when hydrogen is not fully converted, indicating that the ammonia formation rate via the NO_x reduction by H_2 is higher than the ammonia reaction rate with NO_x to form N_2 . In this study, with Pt–Ba/Al, H_2 is detected in the outlet gas during the rich pulses at 300 °C when H_2 , CO or $\text{C}_3\text{H}_6 + \text{CO}_2 + \text{H}_2$ are used as reductant(s), and ammonia is also detected (Fig. 2). On the contrary, no hydrogen is detected using C_3H_6 and the ammonia selectivity tends to be nil. At 400 °C, H_2 is detected in the outlet gas during the rich pulses whatever the considered reducing mixture (results not shown), and the ammonia yield varies between 12% and 65% (Fig. 2). As a reminder, the low ammonia selectivity with Pt/CZ is attributed to the ability of this catalyst to oxidize NH_3 into N_2 , in relation with its oxygen mobility.

To conclude, the real reducing mixture at the catalyst surface during the rich excursions is strongly dependant on the transformation reactions of the introduced reductant(s), which are very sensitive to the support behaviors. At 300 °C, WGS equilibrium and steam reforming are favored over Pt/CZ. As a consequence, whatever the introduced reductant, the reducing mixture on the Pt/CZ catalyst is balanced, especially toward CO and H_2 . Then, the

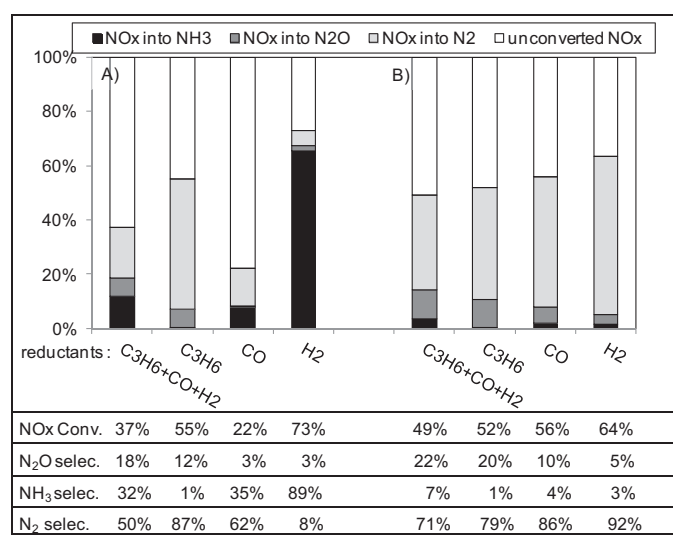


Fig. 7. Comparative effect of the support on NO_x conversion and N-compound selectivities at 300 °C depending on the introduced reductant(s) over (A) Pt–Ba/Al and (B) Pt/CZ catalysts.

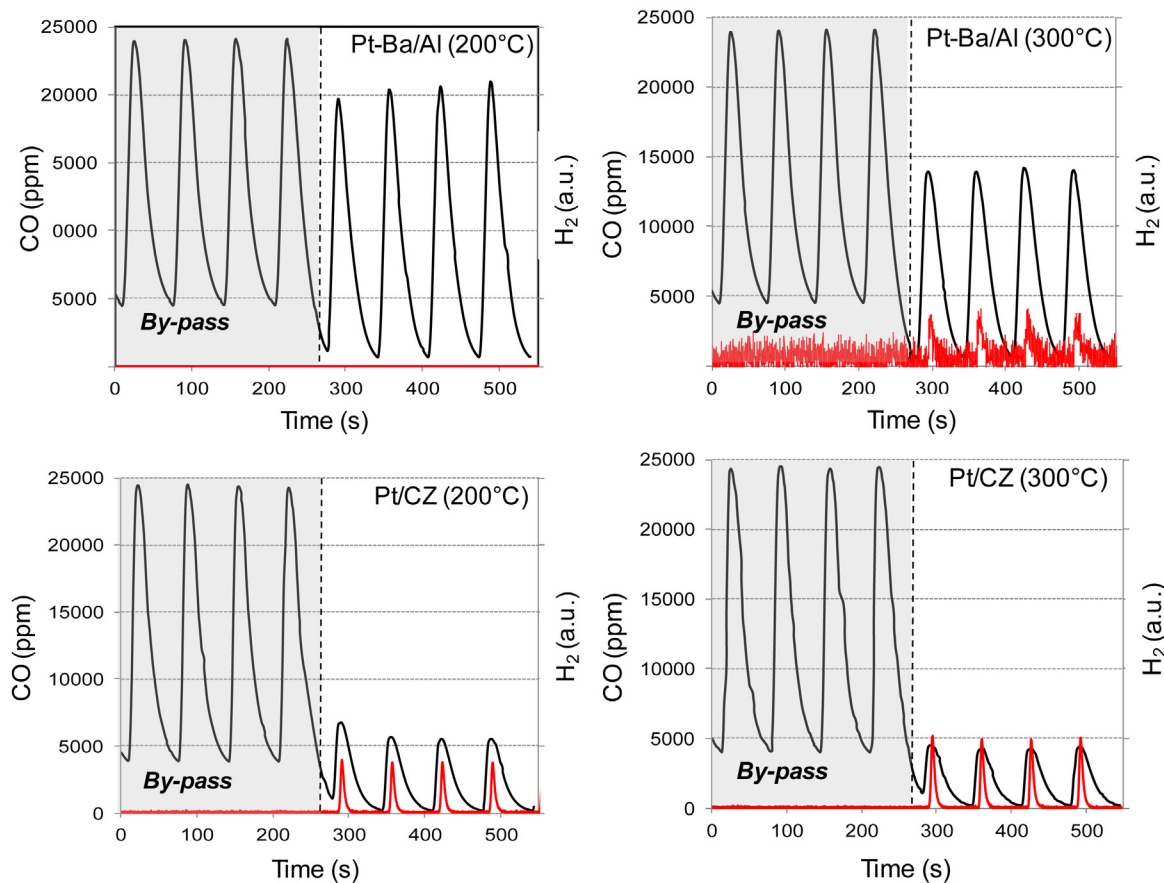


Fig. 8. Evidence of water gas shift (WGS) activity during NSR cycles with CO as reductant. (—), CO; (—), H₂.

observed NO_x conversions are relatively close and vary in a lower extent with Pt/CZ compared with Pt–Ba/Al.

4.3. Comparison of Pt–Ba/Al and Pt/CZ toward N₂O emissions

It was previously reported that the N₂O formation is not only reliable to the excursions in rich atmosphere, but can also be largely produced during the lean periods, depending on reductant. Based on the recorded N₂O profiles during the NSR tests, contributions of both lean and rich phases are detailed in Table 3. In addition to the global NO_x conversion and N₂O selectivity, the N₂O distribution and average N₂O concentrations are reported for both Pt–Ba/Al and Pt/CZ catalysts. The NO_x conversions being rather limited at 200 °C over Pt–Ba/Al, comparison of both catalysts is focused on tests performed at 300 °C.

4.3.1. N₂O emission during the lean periods

At 300 °C, Table 3 shows that the proportion of the N₂O emitted during the lean periods is significantly higher over Pt–Ba/Al when the gas mixtures include C₃H₆, at 71–72% versus 45% for Pt/CZ. These differences are assigned to the higher global N₂O selectivity of Pt/CZ material. Indeed, it is worth noting that the amounts of N₂O emitted during the lean periods are very similar for both catalysts: near 11 ppm using the full gas mixture (C₃H₆ + CO + H₂) or only propylene.

Using only H₂ as reductant, the major part of the N₂O production occurs during the lean phases for both catalysts, at 66% and 60% for Pt–Ba/Al and Pt/CZ, respectively. Again, the amounts of N₂O emitted during the lean atmosphere are very close whatever the support formulation, from 3.4 to 4.7 ppm (Table 3).

With CO as reductant, the N₂O emission during the lean phases is practically nil for both catalysts, because there is no NO_x reduction with CO in excess of O₂ (Fig. 6D). In this case, the global N₂O selectivity observed during NSR cycles depends mainly on the behavior of the catalyst in rich atmosphere. N₂O production is enhanced during the rich pulses over Pt/CZ. This behavior is depicted in Section 4.3.2.

Whatever the chemical nature of considered reductant, and whatever the catalyst, these N₂O concentrations are consistent with results obtained from light-off tests performed only in lean atmosphere, reported in [21] for Pt/CZ. Indeed, similar profiles were obtained with Pt–Ba/Al (Fig. 6) depending on the used reductant(s). The main differences are observed at low temperature with mixtures containing C₃H₆: Pt/CZ is able to convert NO_x at 200 °C, almost only into N₂O, whereas Pt–Ba/Al is inactive at this temperature. However, both catalysts exhibit close N₂O concentrations at 300 °C, in accordance with N₂O concentration reported in Table 3 for the lean periods of the NSR test. In addition, with H₂ as reductant, higher N₂O emissions are detected with Pt/CZ during the test in lean atmosphere. The N₂O concentration is two times higher at 200 °C, and 7 ppm N₂O were still recorded at 300 °C with Pt/CZ, whereas no more NO_x reduction is observed with Pt–Ba/Al (Fig. 6). This result is also in accordance with data reported in Table 3 when only H₂ is used: higher N₂O concentrations were recorded at 200 °C and 300 °C during the lean periods of the NSR tests with Pt/CZ, compared with Pt–Ba/Al.

To summarize, the amounts of nitrous oxides emitted at 300 °C during the lean phases of the NSR test mainly depend on the considered reductant agent, with nearly no influence of the support composition. The variation of the N₂O distribution between both

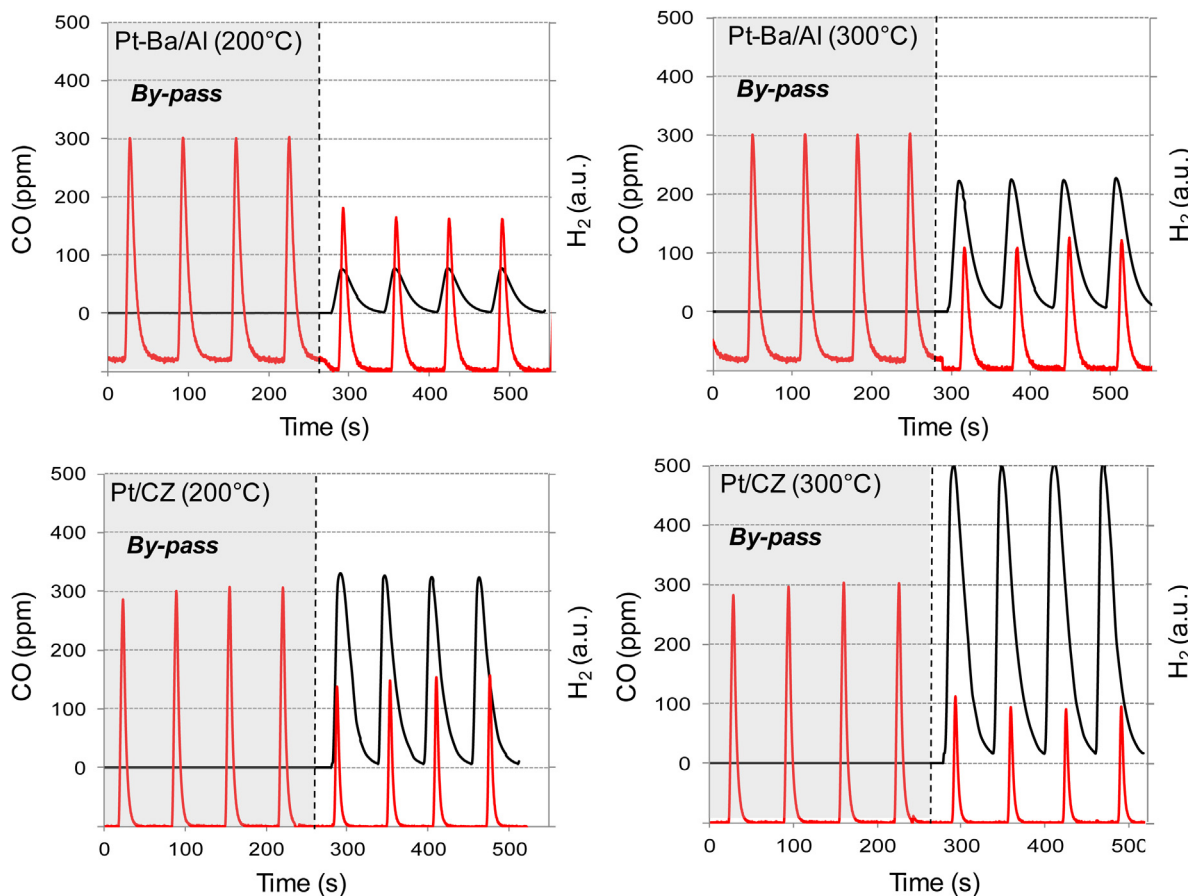


Fig. 9. Evidence of reverse water gas shift (RWGS) activity during NSR cycles with H_2 as reductant. (—), CO; (—), H_2 .

catalysts depends on reactions during the rich pulses, as described in the following part.

4.3.2. N_2O emission during rich pulses

In opposition with N_2O concentrations recorded during the lean periods of the NSR test, N_2O emissions during the rich pulses significantly vary depending on the catalyst. Whatever the reducing mixture, N_2O concentrations are higher on Pt/CZ than on Pt-Al/Ba (Table 3). With gas mixtures containing C_3H_6 (alone or mixed with CO and H_2), the N_2O concentration in the rich pulses is 3 times higher over Pt/CZ, at around 14 ppm versus 4.5 ppm with Pt-Ba/Al.

Differences are even more important using CO, at 12.2 ppm and 1.1 ppm, respectively, but the NO_x conversion is significantly lower on Pt-Ba/Al. Finally, with hydrogen, N_2O concentration in the rich pulses is also higher over Pt/CZ.

Two main hypotheses can be proposed to explain these behaviors. As previously described in Section 4.2, Pt/CZ catalyst strongly favors the transformation of the introduced reductants, leading to a balanced mixture, especially toward CO and H_2 . This phenomenon could explain the very narrow N_2O concentrations recorded in the rich pulses over Pt/CZ for full gas, C_3H_6 and CO as used reductant(s) at 12.2–14.4 ppm. N_2O concentration observed with H_2 is

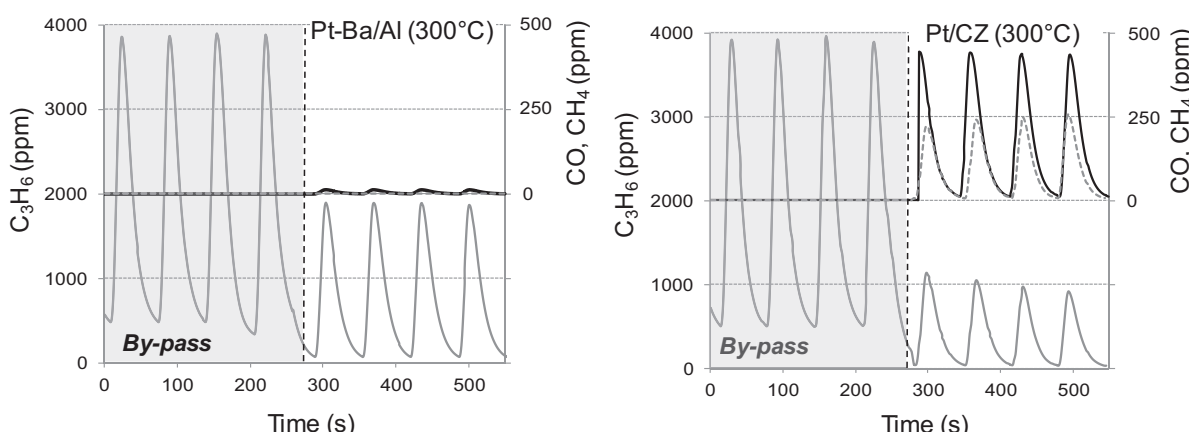


Fig. 10. C_3H_6 (—), CO (—) and CH_4 (***) emission over Pt-Ba/Al and Pt/CZ catalysts at 300 °C during NSR cycles with C_3H_6 as reductant.

lower, but the CO concentration recorded during the rich pulses was relatively low, at around 500 ppm.

However, another phenomenon could participate to the higher N₂O concentration in the rich pulses over Pt/CZ. Indeed, the ceria-based support exhibits a significant oxygen storage capacity [21], which should be associated with a high oxygen mobility (not measured). Taking into accounts that N₂O formation is due to a lack of reduced sites to favor the NO dissociative adsorption, the oxygen mobility of the CZ support may provide oxygen to platinum and favors the N₂O formation. During its own reduction, the support may act as an oxygen tank for platinum. This hypothesis is in accordance with lower N₂O selectivities with the increase of the rich/lean periods length [27], since the relative time in presence oxygen during the rich phases (from support or due to the mix of the rich and lean mixtures) is reduced.

To conclude, the comparison of catalyst formulation in regard to the N₂O formation put in evidence that the amounts of nitrous oxide emitted at 300 °C during the lean mixture are very close depending on the reductant agent studied. The variation of the N₂O distribution between both catalysts mainly depends on reactions during the rich pulses. In this case, both the reductant transformations and the oxygen storage/mobility of the support are supposed to be involved.

5. Conclusion

The influence of the chemical nature of the reductant agent (C₃H₆, CO, H₂ or a mixture of them) was investigated on the NO_x reduction behaviors of a model Pt–Ba/Al catalyst submitted to NSR cycles with complex gas mixtures, including reductant(s) during the lean phases. The influence of the redox properties of the support were studied by comparison with a platinum catalyst supported on reducible based oxide (Pt/CZ). The DeNO_x efficiency and selectivity depend on (i) the temperature, (ii) the chemical nature of the inlet reductant and (iii) the ability of the catalyst to transform the reductant(s).

Generally, over Pt–Ba/Al, the NO_x conversion increases in the 200–400 °C temperature range, but the N₂ selectivity is rather poor due to N₂O emissions at 200–300 °C, and NH₃ emission which tends to increase with temperature.

More precisely, at 200 °C, only the use of hydrogen alone allows a significant NO_x conversion (at 53%), but with a high N₂O selectivity (41%), which is mainly due to the lean DeNO_x activity (for 91%). For comparison, Pt/CZ catalyst is more active at this temperature, with NO_x conversions between 15% and 92% depending on the considered reductant(s), hydrogen still being the more efficient reductant. High N₂O selectivities are also observed over Pt/CZ, especially in presence of propylene. Again, the major part of the N₂O emission is attributable to the NO_x reduction during the lean phases.

At 300 °C, the NO_x conversions vary between 22% and 73% over Pt–Ba/Al with the following order: H₂ > C₃H₆ > C₃H₆ + CO + H₂ > CO. Significant N₂O selectivities are associated with the presence of C₃H₆ in the reaction mixture, with again a large contribution of the lean periods (70%). The NO_x conversions are less dispersed over Pt/CZ (49–64%) depending on the used reductant(s). This behavior is attributed to reductants transformations during rich pulses over Pt/CZ. Indeed, the water gas shift equilibrium and steam reforming reactions are favored on platinum supported over ceria–zirconia-based oxide. The resulting gas mixture is then composed of a large amount of H₂ and CO for this catalyst, whatever the inlet gas composition. Concerning the N₂O emissions, they are very similar during the lean periods for both catalysts, but higher N₂O concentrations are recorded during the rich pulses over Pt/CZ.

In fact, the significant contributions of the lean phases on the global N₂O emissions are consistent with tests performed only in

lean atmosphere in the 200–400 °C temperature range. H₂ leads to N₂O emission for the lowest temperature, C₃H₆ exhibits a N₂O peak near 220–230 °C, and no N₂O emission is observed with CO as reductant in the lean periods.

It was also confirmed in this study that ammonia formation during the rich pulses over Pt–Ba/Al is strongly favors in the presence of unconverted hydrogen, whatever its origin (introduced in the rich mixture or in situ produced), while the catalyst supported over a ceria-based support limits the ammonia emission.

Acknowledgement

The Authors thank the French Ministry of Economy, Finance and Industry for its financial support (FUI contract n° 08 2 90 6669 NOSICA).

References

- [1] W.S. Epling, L.E. Campbell, A. Yezerets, N.W. Currier, J.E. Parks, *Catalysis Reviews: Science and Engineering* 46 (2004) 163–245.
- [2] T. Kobayashi, T. Yamada, K. Kayano, *SAE Technical Papers* 970745 (1997) 63.
- [3] H.L. Fang, H.F.M. DaCosta, *Applied Catalysis B: Environmental* 46 (2003) 17–34.
- [4] M. Eichelbaum, R.J. Farrauto, M.J. Castaldi, *Applied Catalysis B: Environmental* 97 (2010) 90–97.
- [5] F. Birkhold, U. Meingast, P. Wassermann, O. Deutschmann, *Applied Catalysis B: Environmental* 70 (2007) 119–127.
- [6] F.Z. Everton, *Chemical Engineering Science* 64 (2009) 1075–1084.
- [7] M. Koebel, M. Elsener, M. Kleemann, *Catalysis Today* 59 (2000) 335–345.
- [8] M. Koebel, M. Elsener, *Journal of Chromatography A* 689 (1995) 164–169.
- [9] O. Kroeger, M. Elsener, *Chemical Engineering Journal* 152 (2009) 167–176.
- [10] A. Lundstrom, B. Andersson, L. Olsson, *Chemical Engineering Journal* 150 (2009) 544–550.
- [11] G. Piazzesi, O. Kroger, M. Elsener, A. Wokaun, *Applied Catalysis B: Environmental* 65 (2006) 55–61.
- [12] F. Can, X. Courtois, S. Royer, G. Blanchard, S. Rousseau, Daniel Duprez, *Catalysis Today* 197 (2012) 144–154.
- [13] I. Nova, L. Liotti, L. Castoldi, E. Tronconi, P. Forzatti, *Journal of Catalysis* 239 (2006) 244–254.
- [14] Z. Liu, J.A. Anderson, *Journal of Catalysis* 224 (2004) 18–27.
- [15] H. Abdulhamid, E. Fridell, M. Skoglundh, *Topics in Catalysis* 30/31 (2004) 161–168.
- [16] L. Castoldi, I. Nova, L. Liotti, P. Forzatti, *Catalysis Today* 96 (2004) 43–52.
- [17] I. Nova, L. Castoldi, L. Liotti, E. Tronconi, P. Forzatti, *Catalysis Today* 75 (2002) 431–437.
- [18] I. Nova, L. Liotti, P. Forzatti, *Catalysis Today* 136 (2008) 128–135.
- [19] J.-S. Choi, W.P. Partridge, J.A. Pihl, M.-Y. Kim, P. Koci, C.S. Daw, *Catalysis Today* 184 (2012) 20–26.
- [20] E.C. Corbos, M. Haneda, X. Courtois, P. Marecot, D. Duprez, H. Hamada, *Applied Catalysis A: General* 365 (2009) 187–193.
- [21] L. Masdrag, X. Courtois, F. Can, S. Royer, E. Rohart, G. Blanchard, P. Marecot, D. Duprez, *Catalysis Today* 189 (2012) 70–76.
- [22] E.C. Corbos, X. Courtois, F. Can, P. Marécot, D. Duprez, *Applied Catalysis B: Environmental* 84 (2008) 514–523.
- [23] S. Eloussaoui, X. Courtois, P. Marecot, D. Duprez, *Topics in Catalysis* 30/31 (2004) 493–496.
- [24] E.C. Corbos, X. Courtois, N. Bion, P. Marecot, D. Duprez, *Applied Catalysis B: Environmental* 76 (2007) 357–367.
- [25] N. Le Phuc, X. Courtois, F. Can, S. Royer, P. Marecot, D. Duprez, *Applied Catalysis B: Environmental* 102 (2011) 353–361.
- [26] H. Abdulhamid, E. Fridell, M. Skoglundh, *Applied Catalysis B: Environmental* 62 (2006) 319–328.
- [27] U. Elizundia, D. Duraiswami, B. Pereda-Ayo, R. López-Fonseca, J.R. González-Velasco, *Catalysis Today* 176 (2011) 324–327.
- [28] A. Lindholm, N.W. Currier, E. Fridell, A. Yezerets, L. Olsson, *Applied Catalysis B: Environmental* 75 (2007) 78–87.
- [29] T. Szailer, J.H. Kwak, D.H. Kim, J.C. Hanson, C.H.F. Peden, J. Szanyi, *Journal of Catalysis* 239 (2006) 51–64.
- [30] I. Nova, L. Liotti, P. Forzatti, F. Prinetto, G. Ghiootti, *Catalysis Today* 151 (2010) 330–337.
- [31] P. Kočí, F. Plát, J. Štěpánek, Š. Bártová, M. Marek, M. Kubíček, V. Schmeißer, D. Chatterjee, M. Weibel, *Catalysis Today* S147 (2009) S257–S264.
- [32] R. Burch, J.A. Sullivan, T.C. Watling, *Catalysis Today* 42 (1998) 13–23.
- [33] A. Kotsifa, D.I. Kondarides, X.E. Verykios, *Applied Catalysis B: Environmental* 80 (2008) 260–270.
- [34] R. Burch, J.P. Breen, F.C. Meunier, *Applied Catalysis B: Environmental* 39 (2002) 283–303.
- [35] R. Burch, P.J. Millington, *Catalysis Today* 26 (1995) 185–206.
- [36] E. Seker, E. Gulari, *Journal of Catalysis* 194 (2000) 4–13.

- [37] R. Burch, T.C. Watling, *Applied Catalysis B: Environmental* 11 (1997) 207–216.
- [38] C.N. Costa, A.M. Efstatiou, *Applied Catalysis B: Environmental* 72 (2007) 240–252.
- [39] S. Yang, X. Wang, W. Chu, Z. Song, S. Zhao, *Applied Catalysis B: Environmental* 107 (2011) 380–385.
- [40] N. Le Phuc, X. Courtois, F. Can, S. Royer, P. Marecot, D. Duprez, *Applied Catalysis B: Environmental* 102 (2011) 362–371.
- [41] J. Barbier Jr., D. Duprez, *Applied Catalysis B: Environmental* 3 (1993) 61–83.
- [42] N. Le Phuc, X. Courtois, F. Can, S. Berland, S. Royer, P. Marecot, D. Duprez, *Catalysis Today* 176 (2011) 424–428.